

The phase space of the simplest dynamic systems (see equations (1), (3) and (10)) turns out to be remarkably rich in possible realizations of particle dynamics. Regular trajectories that are determined by dynamic invariants always exist. Also, however, there are always stochastic trajectories lacking the corresponding invariant. Stochastic dynamics can arise in exponentially small regions of phase space that are determined by the disturbance parameter given in equation (9). 'Minimal' stochasticity is determined by the minimal region (see equation (12)) and exists for arbitrary disturbances and any number of degrees of freedom >1 . 'Minimal' chaos takes the form of a stochastic web that arises in place of the separatrix net. The net can have various structural quasi-symmetries. Our results suggest the existence of a similar stochastic web in problems of hydrodynamic structures and structural modification of solids.

Received 25 September 1986; accepted 3 February 1987.

1. Fermi, E., *Phys. Rev.* **75**, 1169-1174 (1949).
2. Fermi, E., Pasta, J. R. & Ulam, S. *Studies of Nonlinear Problems* (Los-Alamos Rept LA-1940, 1955).
3. Filonenko, N. N., Sagdeev, R. Z. & Zaslavsky, G. M. *Nuclear Fusion* **7**, 253-266 (1967).
4. Zaslavsky, G. M. & Filonenko, N. N. *Zh. éksp. teor. Fiz.* **54**, 1590-1602 (1968).
5. Arnold, V. I. *Mathematical Methods of Classical Mechanics* (Nauka, Moscow, 1979).
6. Arnold, V. I. *Dokl. Akad. Nauk SSR* **156**, 9-12 (1964).
7. Zaslavsky, G. M. *Zh. éksp. teor. Fiz.* **88**, 1984-1995 (1985).

In particular, a direct correspondence can be established¹² between the web structure illustrated in Fig. 2 and the non-periodic tiling of Penrose³. An example of non-periodic tiling which consists of regular heptagons, fourteen-pointed stars and two additional elements is given in Fig. 6.

One more aspect of equations (3) and (8) is worth mentioning. These equations describe the interaction of two different types of symmetry of particle motion: rotational symmetry due to rotation in magnetic field and translational symmetry along x due to the field of the wave packet. These symmetries cannot be transformed one into another. As a result, for example, the paradox arises of the disappearance of Landau damping in the magnetic field¹⁴. The understanding of many related questions is associated with the nature of the non-trivial interaction of these two types of symmetry.

8. Zaslavsky, G. M. & Chernikov, A. A. *Zh. éksp. teor. Fiz.* **89**, 1632-1647 (1985).
9. Zaslavsky, G. M., Zakharov, M. Yu., Sagdeev, R. Z., Usikov, D. A. & Chernikov, A. A. *Zh. éksp. teor. Fiz.* **91**, 500-516 (1986).
10. Shechtman, D., Blech, I., Gratias, D. & Chan, J. W. *Phys. Rev. Lett.* **53**, 1951-1953 (1984).
11. Nelson, D. R. & Halperin, B. I. *Science* **229**, 233-238 (1985).
12. Zaslavsky, G. M., Zakharov, M. Yu., Sagdeev, R. Z., Usikov, D. A. & Chernikov, A. A. *Pisma Zh. éksp. teor. Fiz.* **44**, 349-353 (1986).
13. Penrose, R. *Bull. Inst. Math. Applics* **10**, 266-271 (1974).
14. Sagdeev, R. Z. & Shapiro, V. D. *Pisma Zh. éksp. teor. Fiz.* **17**, 389-393 (1973).

Tests of the helix dipole model for stabilization of α -helices

Kevin R. Shoemaker*, Peter S. Kim*[†], Eunice J. York[‡], John M. Stewart[‡] & Robert L. Baldwin*

* Department of Biochemistry, Stanford University School of Medicine, Stanford, California 94305, USA

‡ Department of Biochemistry, University of Colorado School of Medicine, Denver, Colorado 80262, USA

Charged groups play a critical role in the stability of the helix formed by the isolated C-peptide (residues 1-13 of ribonuclease A) in aqueous solution. One charged-group effect may arise from interactions between charged residues at either end of the helix and the helix dipole. We report here that studies of C-peptide analogues support the helix dipole model, and provide further evidence for the importance of electrostatic interactions not included in the Zimm-Bragg model for α -helix formation.

THE C-peptide (residues 1-13) and S-peptide (residues 1-20) of RNase A show significant α -helix formation in aqueous solution near 0°C¹⁻³. Nevertheless, predictions of helix stability⁴ based on the Zimm-Bragg equation⁵ and using host-guest data⁶ indicate that helix formation should be negligible for all short peptides (≤ 13 residues), regardless of amino-acid sequence or temperature. Another surprise from studies of helix formation by C-peptide is the charged-group effect: the pH dependence of C-peptide helix content demonstrates the importance of ionizable groups².

Previous work⁴ has shown that the charged-group effect can be assigned to Glu 2⁻ and His 12⁺. This result suggests that interactions with the helix dipole are important. Glu 2⁻ and His 12⁺ are close to the positive and negative poles of the α -helix macrodipole, respectively, and can make favourable charge-dipole interactions that stabilize the helix.

The approach that we have taken is to study analogues of C-peptide that contain single amino-acid substitutions. Two preliminary generalizations can be made⁴: first, single amino-acid substitutions often have a detrimental effect on helix stability, although some which increase helix stability have also

been found; and second, the same amino-acid substitution can have opposite effects on helix stability depending on its location in the helix. With these points in mind, we have designed a C-peptide analogue which shows greater helix stability than C-peptide itself. Other analogues based on this reference peptide have been studied in order first to confirm the importance of Glu 2⁻ and His 12⁺ and then to test the helix dipole model.

Reference peptide with increased helix stability

The sequences of native C-peptide and reference peptide III are given in Fig. 1 legend. Reference peptide III combines two amino-acid substitutions in the C-peptide sequence, Lys 1 \rightarrow acetylAla and Glu 9 \rightarrow Leu, known from earlier work⁴ to increase helix stability. The other two substitutions, Gln 11 \rightarrow Ala and Met 13 \rightarrow Ala, were made for ease of synthesis and purification⁴.

The far-ultraviolet (UV) CD (circular dichroism) spectrum of peptide III under optimal helix-forming conditions (pH 5.2, 3°C) is characteristic of partial helix formation (Fig. 1a). Minima occur at 222 nm (α -helix $n-\pi^*$ transition) and 205 nm (mixture of 2 bands: α -helix $\pi-\pi^*$ transition and random coil $\pi-\pi^*$ transition)⁷. Recent work (ref. 8 and K.R.S. *et al.*, unpublished data) indicates that the change in $[\theta]_{222}$ (mean residue ellipticity at 222 nm) for complete helix formation by C-peptide at 3°C is near 30,000 deg cm² dmol⁻¹, when the baseline value

[†] Present address: Whitehead Institute, Nine Cambridge Center, Cambridge, Massachusetts 02142, USA.

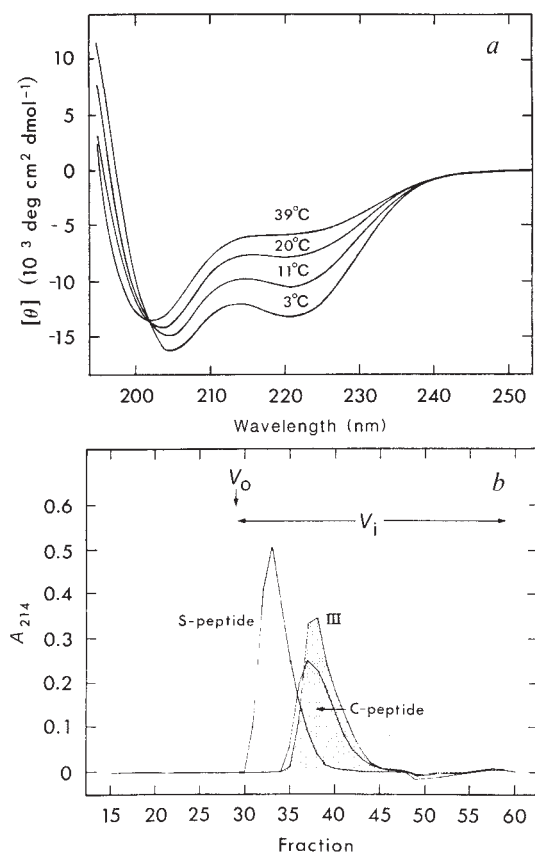


Fig. 1 *a*, Far-UV CD spectra of reference peptide III at various temperatures (pH 5.2, 0.1 M KF). The sequence of native C-peptide, obtained by cyanogen bromide cleavage at Met 13, is Lys-Glu-Thr-Ala-Ala-Ala-Lys-Phe-Glu-Arg-Gln-His-Hse-lactone. The sequence of peptide III is acetyl-Ala-Glu-Thr-Ala-Ala-Ala-Lys-Phe-Leu-Arg-Ala-His-Ala-CONH₂. *b*, Gel filtration chromatography of peptide III (shaded; relative molecular mass M_r 1,398), C-peptide carboxylate (M_r 1,517), and S-peptide(1-19) (M_r 2,095) on Sephadex G-25 superfine. The conditions approximate those used for most CD measurements: 0.1 M NaCl, 1 mM sodium citrate, 1 mM sodium phosphate, 1 mM sodium borate, pH 5.2; 5 °C; peak fraction peptide concentration 20–30 μM . C-peptide has been shown by sedimentation equilibrium to be monomeric in this concentration range¹. Peptide elution was monitored by absorbance at 214 nm. V_0 and V_i mark the void volume and included volume, respectively.

Methods. Peptide synthesis and purification procedures have been described⁴. Both the Stewart Mark V and Biosearch 9500 automatic synthesizers were used. Peptide-resins were acetylated or succinylated with acetic anhydride or succinic anhydride, respectively, in dimethyl formamide containing an equivalent of triethylamine. CD methods were as described^{2,4} and CD spectra were recorded on two instruments: a Jasco J-500A spectropolarimeter in the laboratory of J. T. Yang (University of California Medical School, San Francisco) and an Aviv 60DS spectropolarimeter in the laboratory of P. S. Kim (Whitehead Institute, Cambridge, Massachusetts).

for 0% helix is estimated as +3,000 deg cm² dmol⁻¹. Thus, at pH 5.2 and 3 °C, peptide III shows ~50% helix content, substantially greater than either C-peptide² or reference peptide II⁴.

Figure 1*a* also indicates that the helix formed by peptide III unfolds with increasing temperature. This behaviour has been observed for C-peptide and all analogues studied to date^{2,4}. Two features of these CD spectra are consistent with a helix \leftrightarrow random coil equilibrium: the presence of an isodichroic point at 202 nm and the shift in wavelength of the 205 nm minimum to 201 nm at higher temperatures.

Helix formation by peptide III is monomolecular, as judged by its mobility on a gel filtration column (Fig. 1*b*) and the lack

Table 1 Effect of NH₂-terminal charge on helix content in the absence of Arg 10

NH ₂ -terminal residue	$[\theta]_{222}$ (deg cm ² dmol ⁻¹ ; pH 5.2, 3 °C, 0.1 M NaCl)
succinylAla 1 (-1)	-17,400
acetylAla 1 (0)	-12,600
Ala 1 (+1)	-5,900
Lys 1 (+2)	-4,200

These peptides contain the substitution Arg 10 \rightarrow Ala; otherwise, their sequences after residue 1 are the same as that of reference peptide III (see Fig. 1 legend). Charge of residue 1 in parentheses.

Table 2 Residue frequencies at ends of helices in proteins

NH ₂ -terminus			COOH-terminus		
Residue	<i>P</i>	Rank	Residue	<i>P</i>	Rank
Glu	2.44	1	Lys	1.83	1
Asp	2.02	2	His	1.77	2
His	0.73	11	Arg	1.25	5
Lys	0.66	16	Glu	1.24	6
Arg	0.44	20	Asp	0.61	16

The frequencies of helical boundary residues were obtained from 152 helices in 29 proteins. Adapted from Table VI of ref. 28.

P, normalized frequency of three helical end residues.

of any significant concentration dependence of $[\theta]_{222}$ in the range 10–40 μM (data not shown). The equilibrium between helix and random coil is mobile, and has not reached 100% helix in these studies. Therefore, if the helix were stabilized by oligomer formation, $[\theta]_{222}$ would vary with peptide concentration. Sedimentation equilibrium measurements have shown that C-peptide begins to form aggregates only in a much higher concentration range (>1 mM)¹.

Assignment of the charged-group effect

Figure 2*a* shows pH titrations of helix content for peptide III at 3 °C, where strong helix formation is observed, and at 45 °C, where the helix is largely melted out. In agreement with earlier findings⁴, ionization of either Glu 2 (pH 2 \rightarrow 5) or His 12 (pH 8 \rightarrow 5) results in a sharp increase in helix content. In this peptide, Glu 2 and His 12 are the only groups which titrate in these respective pH ranges. Residue replacement has been used to confirm these assignments: see the notation explained in Fig. 2 legend for peptide III analogues. Peptides III (Glu 2 \rightarrow Ala) and III (His 12 \rightarrow Ala) each show the expected drop in helix content at pH 5.2 and loss of either the acidic or basic branch of the pH titration curve (Fig. 2*b* and *c*)⁹.

To a first approximation, the helix-stabilizing effects of Glu 2⁻ and His 12⁺ are additive, suggesting that they are exerted independently of one another. Approximately the same change in helix content occurs on titrating His 12 in III (Glu 2 \rightarrow Ala) as in peptide III with Glu 2 present, and the same is true of titrating Glu 2 in III (His 12 \rightarrow Ala) as compared to peptide III.

NH₂-terminal charge and helix stability

The helix dipole model explains the charged-group effect by postulating that Glu 2⁻ and His 12⁺ interact with the α -helix dipole and thereby stabilize the helix by position-dependent electrostatic interactions. To test this model, we have varied systematically the charge on the NH₂-terminal residue of reference peptide III, from +2 in Lys 1 (first residue in native C-peptide) to -1 in succinylAla 1. Because solid-phase synthesis¹⁰ proceeds from the COOH-terminus to the NH₂-terminus, it was convenient to split the resin after Glu 2 coupling for addition of different NH₂-terminal residues.

Figure 3*a* shows pH titrations of helix content for these

Fig. 2 The pH dependence of mean residue ellipticity (222 nm) for *a*, reference peptide III, *b*, III (Glu 2→Ala), and *c*, III (His 12→Ala). The measurements were made at 3 °C (●) and 45 °C (○), 0.1 M NaCl. Analogues based on reference peptide III are denoted by giving the substitution: for example, III (Glu 2→Ala) is reference peptide III with alanine in place of Glu 2.

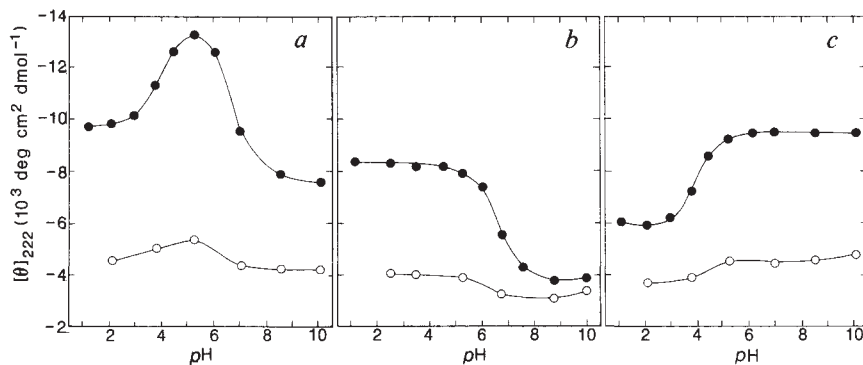
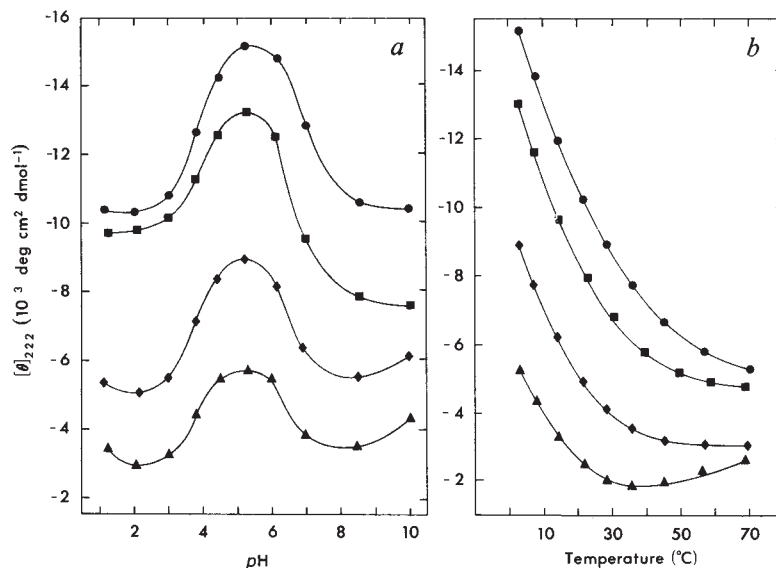


Fig. 3 *a*, The pH dependence of mean residue ellipticity (222 nm) at 3 °C, 0.1 M NaCl for reference peptide III (■), III (acetylAla 1→succinyl Ala) (●), III (acetylAla 1→Ala) (◆), and III (acetylAla 1→Lys) (▲). *b*, Temperature dependence of mean residue ellipticity (222 nm) for the same peptides at pH 5.2, 0.1 M NaCl. Peptides are denoted by the same symbols as in *a*.



peptides at 3 °C. All four peptides have Glu 2 and His 12, and they differ only in the charged residue at the NH₂-terminus. At pH 5.2, where the helix content is maximal and both Glu 2 and His 12 exist in their ionized forms, there is a progressive change in helix content with charge on the NH₂-terminus: succinylAla 1 (-1) > acetylAla 1 (0) > Ala 1 (+1) > Lys 1 (+2). This order of helix content agrees with predictions of the dipole model. As Fig. 3*b* indicates, helix content at 3 °C is correlated with thermal stability of the helix at pH 5.2.

Helix content has also been measured as a function of salt concentration for this set of peptides. Figure 4 shows that helix stability is affected by an electrostatic interaction involving the NH₂-terminus, as the nature of the interaction depends on the NH₂-terminal charge and the interaction is screened by salt. Differences in helix content are largest at low salt concentration. Increasing salt concentration favours helix formation when residue 1 is positively charged (Lys 1), but decreases helix content when residue 1 is negatively charged (succinylAla 1). As interpreted by the helix dipole model, NaCl is screening charge dipole interactions. As expected, the other two peptides in this series show behaviour intermediate between that of the Lys 1 and succinylAla 1 peptides (Fig. 4). Studies with other salts in the Hofmeister series indicate that the effects in this range of salt concentration result chiefly from generalized ion shielding and not specific ion interactions (data not shown).

Studies of peptides with the substitution Arg 10→Ala (manuscript in preparation) indicate that a Glu 2⁻ ··· Arg 10⁺ ion pair, shown clearly in the refined X-ray and neutron crystal structure of intact RNase A¹¹, may also be present in the helix formed by the isolated C-peptide. To determine whether this ion pair is somehow involved in the effect demonstrated here, in which the NH₂-terminal charge strongly affects helix stability,

we have studied a similar set of peptides which contain the additional substitution Arg 10→Ala. Helix contents at pH 5.2, 3 °C, are summarized in Table 1. Both these data and thermal melting profiles (data not shown) indicate that the effect of NH₂-terminal charge is nearly the same in the presence or absence of the postulated Glu 2⁻ ··· Arg 10⁺ ion pair.

Direct ionization at the NH₂ terminus

According to the helix dipole model, direct ionization of charged groups at the NH₂-terminus should affect helix stability. The peptide III (acetylAla 1→Ala, His 12→Ala) contains a free α-NH₂ group. As His 12 also ionizes above pH 5 (*p*K_a ~ 6.7⁴) and thereby alters helix content, His 12 has been replaced by alanine. Figure 5*a* shows pH titration of helix content at 3 °C, which demonstrates the effects of ionization of Glu 2 and the α-NH₂ group. As predicted, helix content increases as the protonated α-NH₂ group loses its positive charge (pH > 6.5).

Similarly, direct ionization of an NH₂-terminal succinyl group was studied in III (acetylAla 1→succinylAla, Glu 2→Ala). Figure 5*b* shows that helix content decreases with protonation of the negatively charged succinyl group. Here, alanine replaces Glu 2, which ionizes with *p*K_a ~ 3.8⁴.

Comparison with other work

Our results strongly support the previous suggestion⁴ that interactions between charged groups and the α-helix macrodipole influence the stability of the helix formed by C-peptide and its analogues. An early indication that these effects are energetically important was provided by the study of Chou and Fasman¹² on the distribution of charged amino acids near the termini of α-helices in proteins. As shown in Table 2, acidic residues occur preferentially near the NH₂-terminus but not near the COOH-

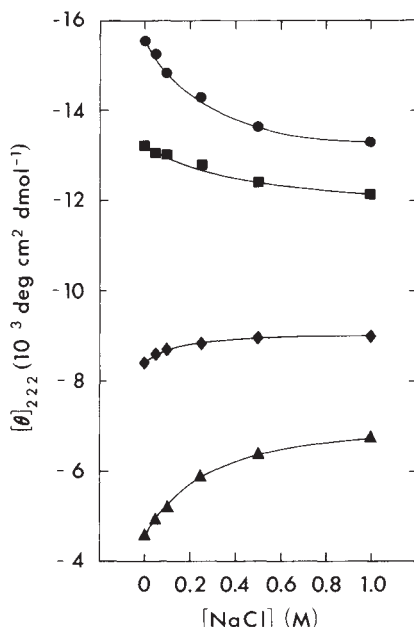


Fig. 4 Salt dependence of mean residue ellipticity (222 nm) at pH 5.2, 3°C for the peptides described in Fig. 3 and denoted by the same symbols. Throughout this range of salt concentration, helix formation remains temperature dependent and occurs in a monomolecular reaction (data not shown).

terminus of α -helices, whereas the reverse is true of basic residues. Blagdon and Goodman¹³ suggested that these findings reflect interactions between the helix dipole and charged residues close to either terminus of an α -helix.

As noted earlier⁴, results from studies of block copolymers by Ooi and coworkers¹⁴ can also be interpreted in terms of a helix dipole model. In their system, helix formation by an (Ala)₂₀ block adjacent to a (Glu⁻)₂₀ block also shows a charged-group effect. For both these block copolymers and for the C-peptide derivatives studied here, the electrostatic effects are sequence-specific. Scheraga¹⁵ notes that sequence-specific interactions, which are not included in the Zimm-Bragg treatment of the helix-coil transition, are either missing or averaged out in the host-guest studies of random copolymers used to determine s and σ values.

Our results support Hol's view¹⁶⁻¹⁸ that interactions between charged groups and the α -helix macrodipole are functionally important in proteins. These interactions are likely to be even larger in proteins than in isolated α -helices in aqueous solution, because the effective dielectric constant in the interior of a protein is believed to be significantly lower than that of bulk water¹⁹. Recently, Perutz and co-workers²⁰ have discussed the possibility that a charged side chain interaction with a helix dipole is responsible for the high pK_a of a histidine residue in haemoglobin (see also ref. 21).

Another example comes from recent studies⁸ of semisynthetic ribonucleases formed by combination of S-protein (residues 21-124) with S-peptide derivatives (residues 1-15). These derivatives, based on the set of C-peptide analogues described here, contain varying NH₂-terminal charge. The results indicate a good correlation between stability of the isolated S-peptide helix and thermal stability of the reconstituted semisynthetic RNase S.

Possible mechanisms for a charged-group effect

By using a new reference peptide that shows good helix formation, we confirm, and demonstrate more decisively than before⁴, that Glu 2⁻ and His 12⁺ are the two charged residues responsible for the pH dependence of C-peptide helix content first noted

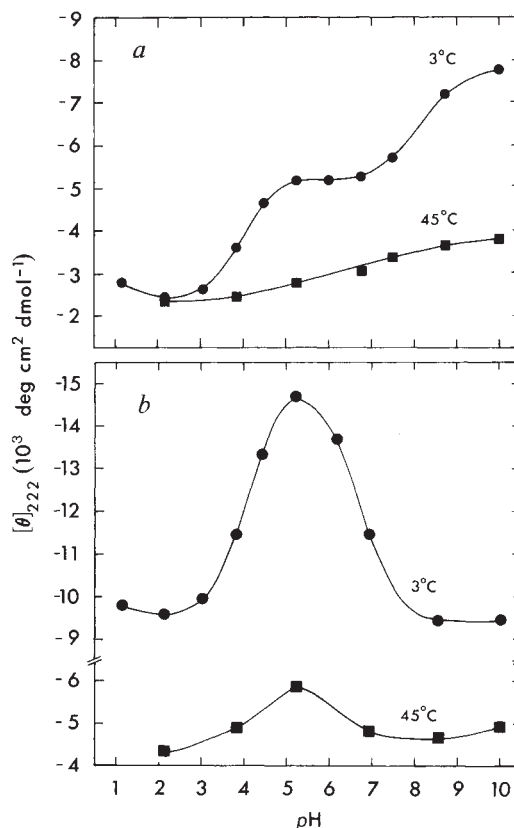


Fig. 5 The pH dependence of mean residue ellipticity (222 nm) for a, III (acetylAla 1 → Ala, His 12 → Ala) and b, III (acetylAla 1 → succinylAla, Glu 2 → Ala). The measurements were made at 3°C (●) and 45°C (■), 0.1 M NaCl.

by Bierzynski *et al.*². This appears to be the major charged-group effect. As Fig. 2 indicates, however, there is residual helix in C-peptide analogues lacking either Glu 2 or His 12 at pH values for which the major charged-group effect is absent. Evidently, these electrostatic interactions do not account for the entire difference between the observed and predicted stabilities of the C-peptide helix⁴.

We introduced the helix dipole model to explain the charged-group effect assigned to Glu 2 and His 12 (ref. 4). In its simplest form, which can be used for making qualitative predictions, the helix dipole model approximates the actual distribution of partial charges in an α -helix as an extended line dipole with a positive pole near the NH₂-terminus of the helix and a negative pole near the COOH-terminus^{16,22}. Thus, electrostatic interactions between one pole of the helix macrodipole and a nearby charged group favour helix formation if the two charges are of opposite sign, and oppose helix formation if they are of like sign⁴.

The charged-group effect was first explained by postulating a Glu 9⁻ ··· His 12⁺ ion pair², but later work ruled out this possibility⁴. Nevertheless, the effects of Glu 2⁻ and His 12⁺ might be explained by mechanisms other than the helix dipole model: both a Glu 2⁻ ··· Arg 10⁺ ion pair and an aromatic interaction between Phe 8 and His 12⁺ have been suggested (ref 23, 29; K.R.S. *et al.*, unpublished data). Such side chain interactions are thought to be generally important for helix stabilization. The long central helices of troponin C and calmodulin may be stabilized by several intrahelical ion pairs and side chain hydrogen bonds²⁴. Glu⁻ ··· Lys⁺ ion pairs contribute to the high stability of helices formed by recently designed model peptides seventeen residues in length (S. Marqusee and R.L.B., manuscript in preparation). Statistical analysis by Maxfield and Scheraga²⁵ indicates that the probability for a charged residue

to be helical is significantly greater if an amino acid of opposite charge is four residues away in the sequence.

In light of other postulated interactions in the C-peptide helix, it is important that we are able to test the helix dipole model here by varying the charge on the NH₂-terminal residue. These studies (Figs 3 and 5) strongly suggest that interactions between a bound charged group and the helix dipole can be important. Screening of these charge-dipole interactions by mobile ions would explain the salt dependences of helix content shown in Fig. 4. More accurate models for making quantitative predictions of these effects will have to consider interactions between the bound charged groups and the point dipoles of individual peptide units. Such a modification of the Zimm-Bragg theory for the helix-coil transition has recently been introduced²⁶.

The charges that are approximated as monopoles in the line dipole model reside primarily at either end of the helix on the four NH and four CO groups that are not hydrogen-bonded. In their discussion of a sulphate-binding protein from *Escherichia coli*, Quiocho and Pflugrath²⁷ note that unsatisfied hydrogen-bonding donor groups at the NH₂-termini of α -helices may account for the binding of negatively charged ligands close to the positive pole of the helix dipole. Two pieces of our data strongly suggest that the effects we observe are due to electrostatic interactions and cannot be explained by hydrogen-

bonding. Both screening of Lys 1²⁺ by NaCl (Fig. 4) and deprotonation of the α -NH₃⁺ group (Fig. 5a) appear to relieve repulsive interactions between bound positive charges and the positive pole of the helix dipole.

Short peptides and side-chain interactions

This work shows that the helix content of C-peptide can be almost doubled by combining a few favourable amino-acid replacements. Thereby, the phenomenon of α -helix formation by short peptides in aqueous solution is changed from a marginally observable experimental system to one that can be readily manipulated and studied. Thus, it is now practical to use short peptides to identify and analyse specific side-chain interactions that influence the stability of isolated α -helices in aqueous solution. Our results suggest that charged-group interactions with the helix dipole may stabilize early intermediates in protein folding.

We thank Virginia MacCosham for technical assistance, Dr S. W. Englander for discussion, Dr J. T. Yang for the use of his spectropolarimeter, and Virginia Sweeney for amino-acid analyses. This research was supported by the NIH (grant number GM 31475). K.R.S. is a predoctoral fellow of the NSF and P.S.K. was a predoctoral fellow of the Medical Scientist Training Program of the NIH.

Received 8 September 1986; accepted 6 February 1987.

1. Brown, J. E. & Klee, W. A. *Biochemistry* **10**, 470-476 (1971).
2. Bierzynski, A., Kim, P. S. & Baldwin, R. L. *Proc. natn. Acad. Sci. U.S.A.* **79**, 2470-2474 (1982).
3. Kim, P. S. & Baldwin, R. L. *Nature* **307**, 329-334 (1984).
4. Shoemaker, K. R. *et al. Proc. natn. Acad. Sci. U.S.A.* **82**, 2349-2353 (1985).
5. Zimm, B. H. & Bragg, J. K. *J. chem. Phys.* **31**, 526-535 (1959).
6. Sueki, M. *et al. Macromolecules* **17**, 148-155 (1984).
7. Holzwarth, G. & Doty, P. *J. Am. chem. Soc.* **87**, 218-228 (1965).
8. Mitchinson, C. & Baldwin, R. L. *Proteins* **1**, 23-33 (1986).
9. Baldwin, R. L. *Trends biochem. Sci.* **11**, 6-9 (1986).
10. Stewart, J. M. & Young, J. D. *Solid Phase Peptide Synthesis* (Pierce Chemical Company, Rockford, Illinois, 1984).
11. Wlodawer, A. & Sjölin, L. *Biochemistry* **22**, 2720-2728 (1983).
12. Chou, P. Y. & Fasman, G. D. *Biochemistry* **13**, 211-221 (1974).
13. Blagdon, D. E. & Goodman, M. *Biopolymers* **14**, 241-245 (1975).
14. Ihara, S., Ooi, T. & Takahashi, S. *Biopolymers* **21**, 131-145 (1982).
15. Scheraga, H. A. *Proc. natn. Acad. Sci. U.S.A.* **82**, 5585-5587 (1985).

16. Hol, W. G. J., van Duijnen, P. T. & Berendsen, H. J. C. *Nature* **273**, 443-446 (1978).
17. Hol, W. G. J., Halie, L. M. & Sander, C. *Nature* **294**, 532-536 (1981).
18. Hol, W. G. J. *Prog. Biophys. molec. Biol.* **45**, 149-195 (1985).
19. Matthew, J. B. A. *Rev. Biophys. Biophys. Chem.* **14**, 387-417 (1985).
20. Perutz, M. F., Gronenborn, A. M., Clore, G. M., Fogg, J. H. & Shih, D. T.-b. *J. molec. Biol.* **183**, 491-498 (1985).
21. Russu, I. M. & Ho, C. *Biochemistry* **25**, 1706-1716 (1986).
22. Sheridan, R. P., Levy, R. M. & Salemme, F. R. *Proc. natn. Acad. Sci. U.S.A.* **79**, 4545-4549 (1982).
23. Rico, M. *et al. Biopolymers* **25**, 1031-1053 (1986).
24. Sundaralingam, M., Drendel, W. & Greaser, M. *Proc. natn. Acad. Sci. U.S.A.* **82**, 7944-7947 (1985).
25. Maxfield, F. R. & Scheraga, H. A. *Macromolecules* **8**, 491-493 (1975).
26. Vasquez, M., Pincus, M. R. & Scheraga, H. A. *Biopolymers* **26**, 351-371 (1987).
27. Pflugrath, J. W. & Quiocho, F. A. *Nature* **314**, 257-260 (1985).
28. Chou, P. Y. & Fasman, G. D. *Adv. Enzym.* **47**, 45-148 (1978).
29. Bierzynski, A., Dadlez, M., Sobocinska, M. & Kupryszewski, G. *Biophys. Chem.* **25**, 127-134 (1986).

LETTERS TO NATURE

Pulsed TeV gamma-rays from Vela X-1

A. R. North, B. C. Raubenheimer, O. C. De Jager,
A. J. van Tonder & G. van Urk

PU-CSIR Cosmic Ray Research Unit, Potchefstroom University,
2520 Potchefstroom, South Africa

Emission of TeV γ -rays from the fast (periods less than 4 s) neutron stars in the X-ray binary systems Cyg X-3, Her X-1 and 4U0115+63 has recently been reported. Here we present the first evidence that the 283-s neutron star in the X-ray binary Vela X-1 radiates steady, pulsed TeV γ -rays with a sinusoidal light curve. This is also the first evidence that a wind-driven binary system radiates in this energy range. A periodic enhancement was also observed which was in phase with the steady pulsed emission and eight times stronger. This event was directly observable as an enhancement in the counting rate of the telescope and occurred while the pulsar was entering eclipse. This is considered to be an indication that the enhancement was caused by γ -ray production by a charged-particle beam interacting with the limb of the companion star. This fact further indicates that TeV γ -rays are not produced on the neutron star itself but in the accreting material in the system. This is probably the case with some of the other observed binaries.

The binary X-ray source Vela X-1 was discovered by the Uhuru and SAS 3 satellites¹ during 1975 and has been continuously monitored since then by a variety of satellites^{2,3}. The optical counterpart was identified⁴ as the B supergiant HD77581 at distance of (1.9 ± 0.2) kpc from the Earth. The orbital period is (8.9649 ± 0.002) days² whilst the pulse period of the neutron star is (282.84 ± 0.10) s. The X-ray emission as a function of orbital phase shows rapid and complicated variations as may be expected from a wind-driven, accreting binary^{1,3}. Large secular variations in the pulse period over timescales of days and years have been observed² but from 1980 to 1984 only a small spin-up ($\dot{P}/P = -2 \times 10^{-5} \text{ yr}^{-1}$) is evident³. The pulsed light curve is highly variable in the X-ray region changing from a very broad structure with five discernible peaks in the 5 keV range⁵ to a broad double peak in the (15-30) keV range^{2,6}. Vela X-1 was also reported to radiate in the PeV energy range^{7,8}.

Observations of Vela X-1 were made on eleven nights during the period from 2 April to 10 May 1986 with the TeV γ -ray telescope at Potchefstroom^{9,10}. This telescope is based on the atmospheric Cerenkov technique with a threshold energy of 1 TeV at the zenith and a field of view of 2.2°. On all occasions the source was tracked for a period of between 95 and 190 minutes at zenith angles between 17° and 36°, (observations at larger zenith angles were excluded due to the strong zenith angle dependence of the count rate). A total number of 54,450 Cerenkov events were registered during the observation time of 26.2 hours. The arrival time of each event was registered with a